Using CERES Data to Evaluate the Infrared Flux Derived From Diffusivity Approximation

Wenbo Sun, Yongxiang Hu, Norman G. Loeb, Bing Lin, and Martin G. Mlynczak

Abstract—Based on the diffusivity approximation theory, the infrared flux at the top of atmosphere (TOA) can be obtained by multiplying a factor of π on the infrared radiance that was measured at a viewing zenith angle (VZA) of 53°. This letter applies the diffusivity approximation on radiance measurements of the Clouds and the Earth's Radiant Energy System (CERES) to derive TOA infrared fluxes and compares these fluxes with the state-of-the-art CERES outgoing radiative fluxes. We find that the mean difference between the two kinds of instantaneous flux that were estimated at the window channel is ~ 1 W $\cdot$ m^{-2}, with a root-mean-square error of ~ 1.7 W $\cdot$ m^{-2}. This result shows that radiance measurement at a fixed VZA of 53° is a simple and effective method in the remote sensing of the infrared flux for satellite missions that monitor some specific climate processes and require longwave/window TOA fluxes, such as the Broad Band Radiometer instrument on EarthCARE; however, this approach may involve errors from an inhomogeneous scene or non-Lambertian emission of the surface. A careful design of the VZA and scan mode, such as a conical scan at 53°, would produce much more convenient infrared flux measurements for the Earth–atmosphere system than other designs.

Index Terms—Clouds and the Earth's Radiant Energy System (CERES), diffusivity approximation, infrared flux.

I. Introduction

THE OUTGOING longwave flux (OLF), which cools the Earth–atmosphere system, is a critical factor in determining the Earth's climate. The OLF is measured globally through satellite remote sensing. Spaceborne instruments measure the radiances instead of fluxes. One of the challenges that are involved in the satellite remote sensing for the Earth's radiation budget is the conversion of measured radiances to radiative fluxes. Suttles *et al.* [10] have shown that the process of radiance-to-flux conversion was a major error source in the Earth Radiation Budget Experiment [1]. To infer fluxes from radiance measurements, a standard procedure is to use empirical angular distribution models (ADMs) to convert radiances into fluxes [7], [8]. By developing new empirical ADMs from the Clouds and the Earth's Radiant Energy System (CERES) [12], [13] broadband radiance measurements and the Moderate Resolution Imaging Spectroradiometer (MODIS) [6] cloud property retrievals [7], the CERES experiment has significantly improved the accuracy of satellite-derived top-of-atmosphere (TOA) fluxes [8].

To build the state-of-the-art CERES longwave/window ADMs for a high global longwave flux accuracy of ~ 0.35 W $\cdot$ m^{-2}, the CERES employs various scan modes that cover a wide range of viewing angles [13]. These scan modes and viewing angles cannot be achieved by satellite missions that monitor some specific climate processes and require longwave/window TOA fluxes, such as the Broad Band Radiometer (BBR) on the Earth Clouds, Aerosols and Radiation Explorer (EarthCARE) satellite of the European Space Agency (ESA) [2]. Scheduled for launch in 2012, the ESA's EarchCARE BBR will make radiance measurements at three along-track viewing angles of 55° fore and aft plus nadir. The optimized viewing angles for the measurement of shortwave and longwave fluxes are different [3]. Designed to work for a broadband flux, the BBR viewing angles seem to be a compromise for shortwave and longwave fluxes. Therefore, the BBR also requires ADMs for the radiance-to-flux conversion. The ADMs for the EarthCARE BBR are derived by using TOA radiances and fluxes that are simulated by the Monte Carlo photon transport algorithm in the EarthCARE Simulator.

As an alternate method for remote sensing of the longwave flux, the OLF can be estimated by multiplying a factor of π on the infrared radiance that is measured at a "sweet-spot" viewing zenith angle (VZA) of 53°, based on the diffusivity approximation [4]. In this letter, we apply the diffusivity approximation to the CERES window-channel [window (WN): 8–12 μm] radiances at the VZA of 53° to calculate the WN OLF and compare with the CERES product that was obtained from applying the CERES ADMs to the WN radiances. In Section II, we will give a brief review of the simple method for OLF based on the diffusivity approximation. In Section III, we will show a model validation of the diffusivity approximation algorithm and examine the accuracy of the OLF from this method with the OLF from the CERES ADMs. Summary and conclusions are given in Section IV.

II. Diffusivity Approximation for Infrared Flux Calculation

For infrared emission from the Earth–atmosphere system, the upward flux for a band $\Delta\nu$ can be expressed as

$$F_{\nu}^{\uparrow}\left[\tau_{\bar{\nu}}(p, p_s)\right] = \pi B_{\bar{\nu}}(\theta_s) T_{\bar{\nu}}^{f}\left[\tau_{\bar{\nu}}(p, p_s)\right]$$
$$+ \int_{p_s}^{p} \pi B_{\bar{\nu}}(\theta') \frac{\partial T_{\bar{\nu}}^{f}\left[\tau_{\bar{\nu}}(p, p')\right]}{\partial p'} dp' \quad (1)$$

W. Sun is with the Center for Atmospheric Sciences, Hampton University, Hampton, VA 23668 USA. He is also with the NASA Langley Research Center, Hampton, VA 23681 USA (e-mail: w.sun@larc.nasa.gov).

Y. Hu, N. G. Loeb, B. Lin, and M. G. Mlynczak are with the NASA Langley Research Center, Hampton, VA 23681 USA.

where $B_{\bar{\nu}}(\theta)$ denotes the blackbody emission at temperature θ, p_s is the surface pressure, θ_s is the surface temperature, θ' is the temperature at pressure p', and $T_{\bar{\nu}}^f[\tau_{\bar{\nu}}(p, p')]$ is the flux transmittance that was defined in terms of the optical depth $\tau_{\bar{\nu}}(p, p')$ for a slab of atmosphere between p and p'. For least mean errors under all-sky conditions, the flux transmittance $T_{\bar{\nu}}^f[\tau_{\bar{\nu}}(p, p')]$ is related to transmittance $T_{\bar{\nu}}[\tau_{\bar{\nu}}(p, p')]$ by a diffusivity factor of 1.66 as

$$
\begin{aligned}
T_{\bar{\nu}}^f[\tau_{\bar{\nu}}(p, p')] &= T_{\bar{\nu}}[1.66\tau_{\bar{\nu}}(p, p')] \\
&= T_{\bar{\nu}}[\tau_{\bar{\nu}}(p, p')/\cos(53°)]. \quad (2)
\end{aligned}
$$

Therefore, (1) can be rewritten as

$$
\begin{aligned}
F_{\bar{\nu}}^{\uparrow}[\tau_{\bar{\nu}}(p, p_s)] = \pi \Bigg\{ &B_{\bar{\nu}}(\theta_s) T_{\bar{\nu}}[\tau_{\bar{\nu}}(p, p')/\cos(53°)] \\
&+ \int_{p_s}^{p} B_{\bar{\nu}}(\theta') \frac{\partial T_{\bar{\nu}}[\tau_{\bar{\nu}}(p, p')/\cos(53°)]}{\partial p'} dp' \Bigg\}. \quad (3)
\end{aligned}
$$

In (3), the quantity within { } is exactly the radiance at the VZA of 53°. Therefore, the infrared flux at TOA can be obtained by multiplying a factor of π on the infrared radiance that was measured at a VZA of 53°.

III. RESULT

To validate the diffusivity approximation algorithm for OLF with a model simulation, we use the DIScrete Ordinate Radiative Transfer (DISORT) model [9] for a layer of plane-parallel cloud over a Lambertian surface to generate a series of infrared radiances at 53°. At the same time, the radiances at 128 zenith angles and 36 azimuth angles are integrated to produce upward fluxes. As an initial study, we choose the atmospheric window band (WN: 8–12 μm) to do the simulation to avoid the complicated gas absorption treatment in the DISORT. Fig. 1(a) shows the comparison of the fluxes from the diffusivity approximation and those from direct integration of the radiances over the upper half-space. The surface temperature is assumed to be 290 K, and the cloud temperature is assumed to vary linearly from 290 K at the cloud bottom to 260 K at the cloud top. The cloud layer optical depth is assumed to be 0 to 10 with an increment of 0.1. The single-scattering albedo of the cloud is assumed to be 0.4. The phase function of the cloud is calculated with the Legendre polynomial expansion of the Henyey–Greenstein phase function, i.e., $p(\mu) = \sum_{k=0}^{128}[(2k+1)g^k P_k(\mu)]$, where $P_k(\mu)$ is the kth-degree Legendre function in terms of the cosine of scattering angle μ, and the asymmetry factor g is set to be 0.5. We can see that the simulated fluxes from the diffusivity approximation at 53° and direct integration are very close. The linear regression line for the two kinds of fluxes has a slope of 1.01 and an intercept of -1.6 W $\cdot$ m^{-2}. The coefficient of determination is 0.999, which means a nearly perfect correlation. Furthermore, as a sensitivity study, Fig. 1(b) shows the WN flux differences between actual values and those from diffusivity approximations at VZAs of 50°, 53°, and 56°, respectively, as functions of WN flux (which correlates with optical thickness). We can see that, for different fluxes (or optical thickness), diffusivity approximation at different
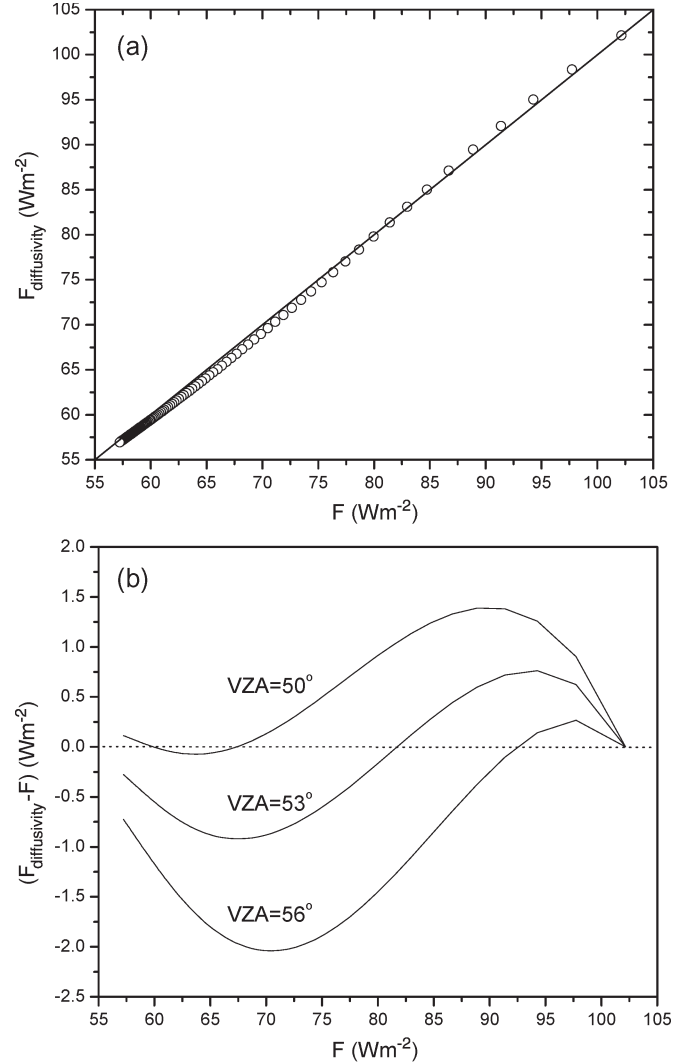

Fig. 1. (a) Comparison of the fluxes from the diffusivity approximation $F_{\text{diffusivity}}$ and those from direct integration of the radiances over the upper half-space from a radiative transfer simulation F. Also shown is the linear regression curve between the fluxes and (b) the WN broadband flux differences between actual values and those from diffusivity approximations at VZAs of 50°, 53°, and 56°, respectively, as functions of WN flux.

angles shows different accuracies. This is consistent with the suggestion that the diffusivity factor varies with optical depth [11]. However, it is obvious that the diffusivity approximation at 53° produces the least error (< 1 W $\cdot$ m^{-2} instantaneously) for all-sky conditions.

For actual atmospheric conditions, more factors could be involved in the estimated errors than what a simple model could account for, such as the effect of inhomogeneous scene and non-Lambertian emission of the surface. These may cause the fluxes that were calculated by diffusivity approximation to deviate from actual values. This is examined as follows.

We use all CERES WN measurements in January 2005 to check the accuracy of the diffusivity approximation. The WN radiances and fluxes from the CERES SSF dataset [5] with VZAs between 52.9° and 53.05° are used. Because the CERES ADMs produce very small errors in all viewing angles [7], the fluxes that were converted from the 53° radiances by the ADMs should be accurate enough for evaluation of the diffusivity approximation. Fig. 2 shows the histograms of the difference
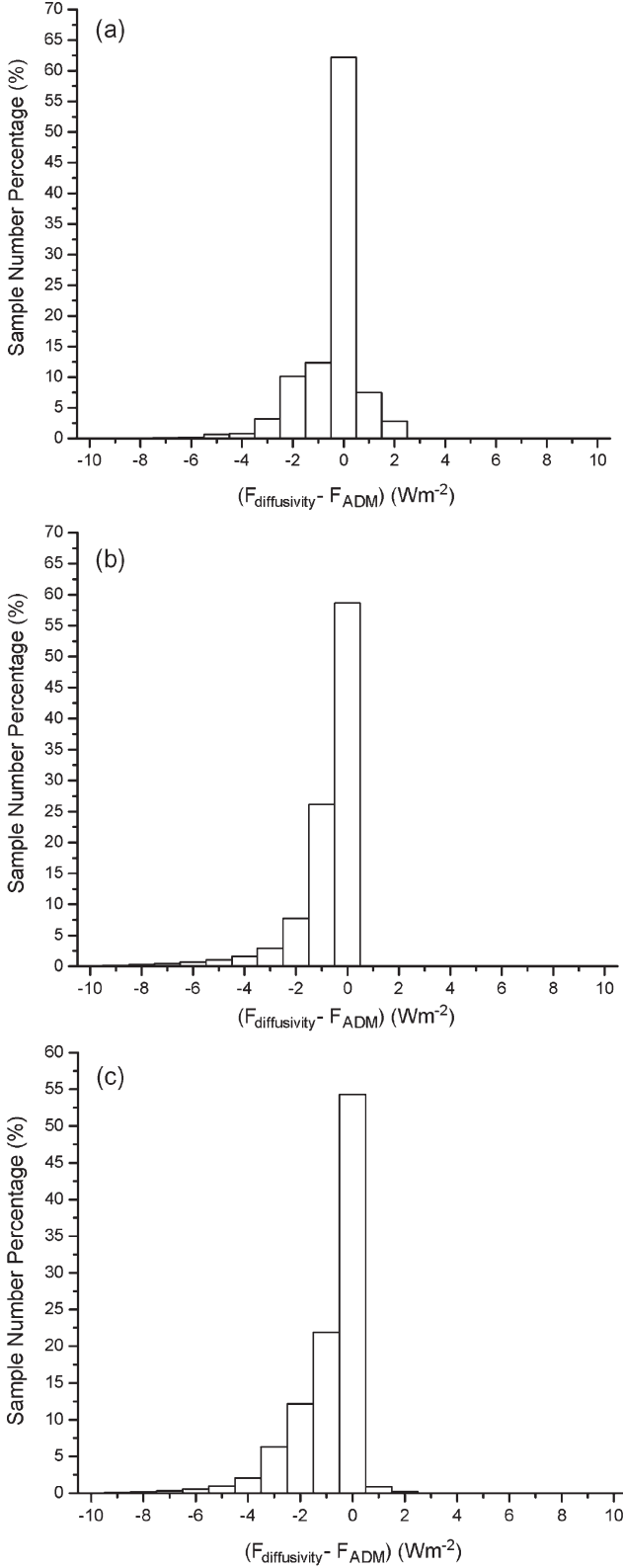
Fig. 2. Histograms of the differences between the window-channel fluxes from the diffusivity approximation and CERES ADMs (i.e., $F_{\text{diffusivity}} - F_{\text{ADM}}$) for the (a) clear-sky (cloud coverage $\leq 1\%$), (b) overcast-cloud (cloud coverage $\geq 99\%$), and (c) all-sky ($100\% \geq$ cloud coverage $\geq 0\%$) conditions for 31 days of January 2005 between $75°$ S and $75°$ N.
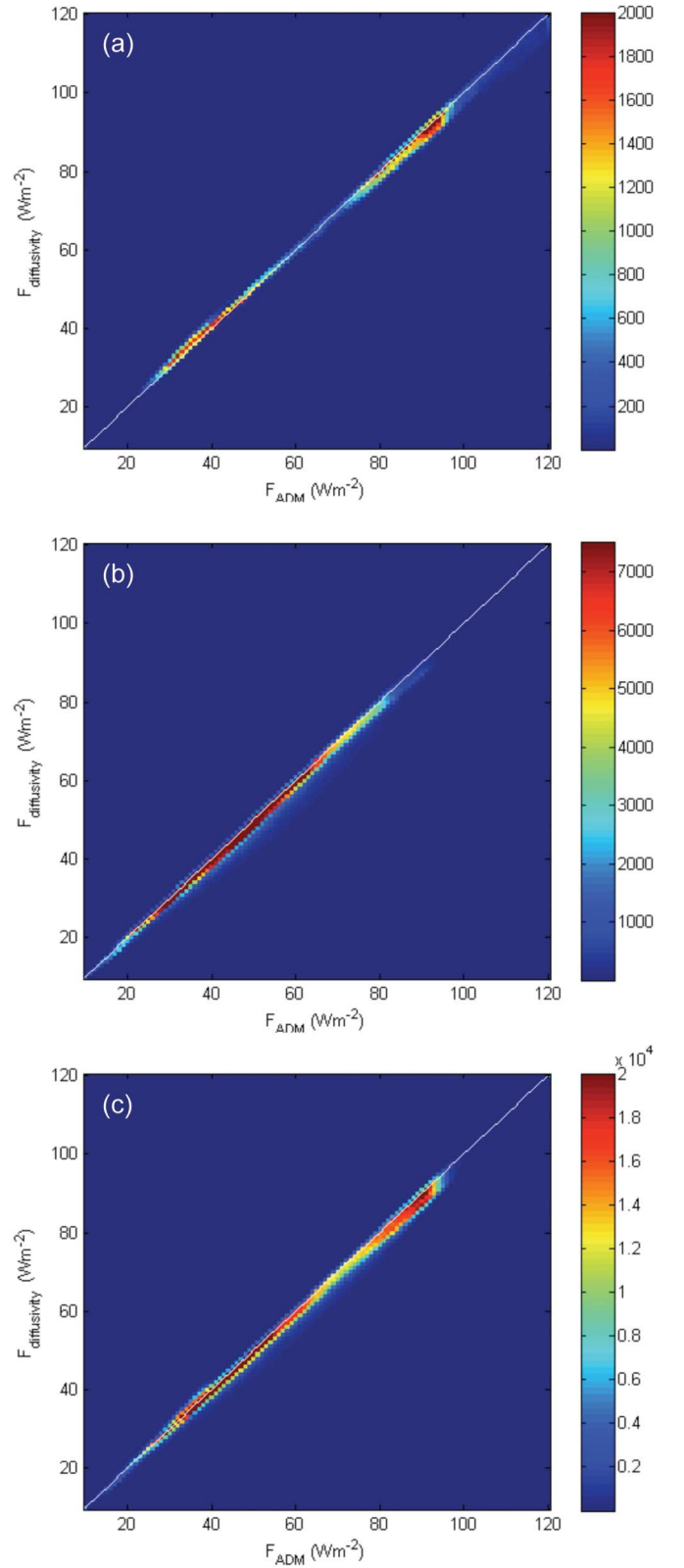
Fig. 3. Comparisons of the window fluxes for the (a) clear-sky, (b) overcast-cloud, and (c) all-sky conditions, from the diffusivity approximation theory and CERES window ADMs for 31 days of January 2005 between $75°$ S and $75°$ N. The color bar shows the occurrence frequency of the samples.

between the WN fluxes for the clear-sky [cloud coverage $\leq 1\%$, Fig. 2(a)], overcast-cloud [cloud coverage $\geq 99\%$, Fig. 2(b)],

and all-sky [$100\% \geq$ cloud coverage $\geq 0\%$, Fig. 2(c)] conditions, from the diffusivity approximation and CERES WN
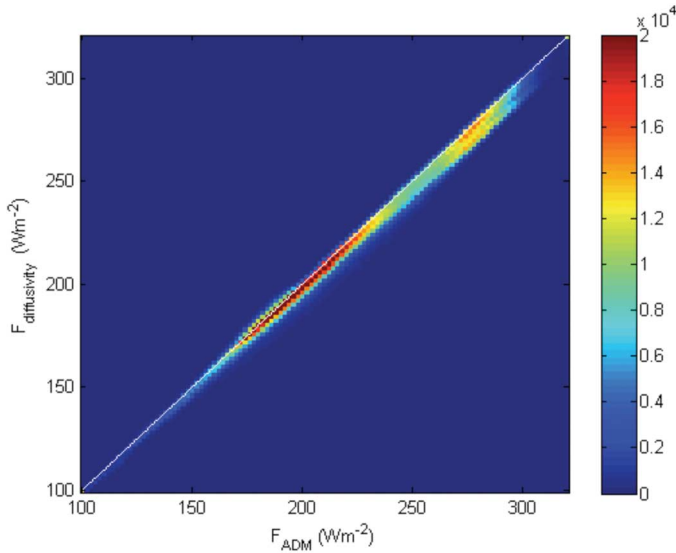
Fig. 4. Comparison of the all-sky total longwave fluxes from the diffusivity approximation theory and CERES ADMs for 31 days of January 2005 between 75° S and 75° N. The color bar shows the occurrence frequency of the samples.

ADMs (i.e., $F_{\text{diffusivity}} - F_{\text{ADM}}$) for 31 days of January 2005. Note that, because the cloud coverage retrieval from the MODIS for polar winter is not reliable, the comparison is limited within the zone between 75° S and 75° N. We can see that, for all cases, the peaks of the distribution occur at a flux difference of ~ 0 W $\cdot$ m^{-2}, with $\sim 90\%$ of the population between ± 2 W $\cdot$ m^{-2}. For the clear-sky condition, the monthly mean difference between the two fluxes is only -0.37 W $\cdot$ m^{-2}, with a root-mean-square (rms) difference between the instantaneous fluxes of ~ 1.49 W $\cdot$ m^{-2}. For both the overcast-cloud and all-sky cases, the monthly mean differences are about -1.0 W $\cdot$ m^{-2}, with a rms difference of ~ 1.7 W $\cdot$ m^{-2}. The corresponding comparisons of the WN fluxes for these cases are shown in Fig. 3. We can see that the two results have excellent agreement. This means that, for the window band, the diffusivity approximation can produce accurate fluxes. These demonstrate that the CERES WN data do support the "sweet-spot" theory.

We also compare the total longwave fluxes of the all-sky case from the diffusivity approximation and CERES ADMs for 31 days of January 2005. Fig. 4 shows that these fluxes also agree well. Only when fluxes are large ($> \sim 250$ W $\cdot$ m^{-2}) is there a branch of samples that slightly deviate from most population. The reason for this deviation is not clear. It may be because inhomogeneous scenes such as broken clouds or mixed scene types on the surface cause errors in the diffusivity approximation. It may also be because the CERES ADMs are applied to the wrong scene types involving undetected broken or thin clouds. In summary, the diffusivity approximation theory can potentially be applied to derive total longwave fluxes, but systematic validations need to be done based on both model simulations and measurement data analyses.

IV. SUMMARY AND CONCLUSION

In this letter, the TOA infrared flux derived from satellite radiance measurements using diffusivity approximation is eval-

uated through the data that were obtained from applying the CERES ADMs to the same radiance measurements. We find that, for over 90% of the measurements, the instantaneous difference between the CERES WN flux and that derived from the diffusivity approximation is within ± 2 W $\cdot$ m^{-2}; the mean difference is smaller than ~ 1 W $\cdot$ m^{-2}, with a rms difference of less than ~ 1.7 W $\cdot$ m^{-2}. This result shows that the radiance measurement at the fixed VZA of 53° is a simple and effective method in the remote sensing of the infrared flux for satellite missions that monitor some specific climate processes and require longwave/window TOA fluxes, such as the BBR instrument on EarthCARE. A careful design of the VZA and scan mode, such as a conical scan at 53°, would produce much more convenient infrared flux measurements for Earth–atmosphere systems than other designs.

REFERENCES

[1] B. R. Barkstrom, "The Earth radiation budget experiment (ERBE)," *Bull. Amer. Meteorol. Soc.*, vol. 65, no. 11, pp. 1170–1186, Nov. 1984.
[2] J.-L. Bezy, W. Leibrandt, A. Heliere, P. Silvestrin, C.-C. Lin, P. Ingmann, T. Kimura, and H. Kumagai, "The ESA Earth explorer Earth-CARE mission," *Proc. SPIE*, vol. 5882, pp. 58820F.1–58820F.12, 2005.
[3] A. Bodas-Salcedo, J. F. Gimeno-Ferrer, and E. Lopez-Baeza, "Flux retrieval optimization with a nonscanner along-track broadband radiometer," *J. Geophys. Res.*, vol. 108, no. D2, pp. AAC8.1–AAC8.12, 2003. DOI:10.1029/2002JD002162.
[4] W. M. Elsasser, "Heat transfer by infrared radiation in the atmosphere," in *Harvard Meteorological Studies*, vol. 6. Cambridge, MA: Harvard Univ. Press, 1942, p. 107.
[5] E. B. Geier, R. N. Green, D. P. Kratz, P. Minnis, W. F. Miller, S. K. Nolan, and C. B. Franklin, *Single Satellite Footprint TOA/Surface Fluxes and Clouds (SSF) Collection Document*, 2001. [Online]. Available: http://asd-www.larc.nasa.gov/ceres/ASDceres.html
[6] M. D. King, Y. J. Kaufman, W. P. Menzel, and D. Tanre, "Remote sensing of cloud, aerosol, and water vapor properties from the moderate resolution imaging spectrometer (MODIS)," *IEEE Trans. Geosci. Remote Sens.*, vol. 30, no. 1, pp. 2–27, Jan. 1992.
[7] N. G. Loeb, S. Kato, K. Loukachine, and N. Manalo-Smith, "Angular distribution models for top-of-atmosphere radiative flux estimation from the clouds and the Earth's radiant energy system instrument on the terra satellite. Part I—Methodology," *J. Atmos. Ocean. Technol.*, vol. 22, no. 4, pp. 338–351, Apr. 2005.
[8] N. G. Loeb, S. Kato, K. Loukachine, N. Manalo-Smith, and D. R. Doelling, "Angular distribution models for top-of-atmosphere radiative flux estimation from the clouds and the Earth's radiant energy system instrument on the terra satellite. Part II—Validation," *J. Atmos. Ocean. Technol*, vol. 24, no. 4, pp. 564–584, Apr. 2007.
[9] K. Stamnes, S. C. Tsay, W. J. Wiscombe, and K. Jayaweera, "Numerically stable algorithm for discrete-ordinate-method radiative transfer in multiple scattering and emitting layered media," *Appl. Opt.*, vol. 27, no. 12, pp. 2502–2509, Jun. 1988.
[10] J. T. Suttles, B. A. Wielicki, and S. Vemury, "Top-of-atmosphere radiative fluxes: Validation of ERBE scanner inversion algorithm using Nimbus-7 ERB data," *J. Appl. Meteorol.*, vol. 31, no. 7, pp. 784–796, Jul. 1992.
[11] D. S. Turner, "Systematic errors inherent in the current modeling of the reflected downward flux term used by remote sensing models," *Appl. Opt.*, vol. 43, no. 11, pp. 2369–2383, Apr. 2004.
[12] B. A. Wielicki, B. R. Barkstrom, E. F. Harrison, R. B. Lee, III, G. L. Smith, and J. E. Cooper, "Clouds and the Earth's Radiant Energy System (CERES): An Earth observing system experiment," *Bull. Amer. Meteorol. Soc.*, vol. 77, no. 5, pp. 853–868, May 1996.
[13] B. A. Wielicki, B. R. Barkstrom, B. A. Baum, T. P. Charlock, R. N. Green, D. P. Kratz, R. B. Lee, P. Minnis, G. L. Smith, T. Wong, D. F. Young, R. D. Cess, J. A. Coakley, D. A. H. Crommelynck, L. Donner, R. Kandel, M. D. King, A. J. Miller, V. Ramanathan, D. A. Randall, L. L. Stowe, and R. M. Welch, "Clouds and the Earth's Radiant Energy System (CERES): Algorithm overview," *IEEE Trans. Geosci. Remote Sens.*, vol. 36, no. 4, pp. 1127–1141, Jul. 1998.